**Atmospheric
Chemistry
and Physics**

Temporal variations of black carbon in Guangzhou, China, in summer 2006

R. L. Verma[1], L. K. Sahu[1], Y. Kondo[1], N. Takegawa[1], S. Han[1], J. S. Jung[2], Y. J. Kim[2], S. Fan[3], N. Sugimoto[4], M. H. Shammaa[1], Y. H. Zhang[5], and Y. Zhao[6]

[1]Research Center for Advanced Science and Technology, University of Tokyo, Tokyo, Japan
[2]Advanced Environmental Monitoring Research Center, Department of Environmental Science and Engineering, Gwangju Institute of Science and Technology (GIST), Gwangju, Republic of Korea
[3]Institute of Environmental Meteorology, School of Environmental Science and Engineering, Sun Yat-sen University, Guangzhou, China
[4]Atmospheric Remote Sensing Section, National Institute for Environmental Studies, Tsukuba, Japan
[5]State Key Joint Laboratory of Environmental Simulation and Pollution Control, College of Environmental Science and Engineering, Peking University, Beijing, China
[6]Air Quality Research Center, University of California, Davis, USA

Abstract. In situ measurements of the mass concentration of black carbon (BC) and mixing ratios of carbon monoxide (CO) and carbon dioxide (CO_2) were made at Guangzhou, an urban measurement site in the Pearl River Delta (PRD), China, in July 2006. The average ± standard deviation (SD) concentrations of BC, CO, and CO_2 were $4.7\pm2.3\,\mu g C\,m^{-3}$, 798 ± 459 ppbv, and 400 ± 13 ppmv, respectively. The trends of these species were mainly controlled by synoptic-scale changes in meteorology during the campaign. Based on back trajectories, data are analyzed separately for two different air mass types representing northerly and southerly flows. The northerly air masses, which constituted ∼25% of the campaign, originated mostly in the PRD and hence represent observations on regional scales. On the other hand, during southerly flow (∼75%), the measurements were influenced by dilution due to cleaner marine air. The diurnal patterns of BC, CO, and CO_2 exhibited peak concentrations during the morning and evening hours coinciding with rush-hour traffic. The ratios of OC/BC were lower during the morning hour peaks in the concentrations of primary pollutants due to their fresh emissions mainly from vehicular traffic in Guangzhou. The diurnal variations of BC observed in southerly air masses tended to follow the traffic patterns of heavy-duty vehicles (HDV) in Guangzhou, while the roles of other sources need to be investigated. The slopes of $\Delta BC/\Delta CO$, $\Delta BC/\Delta CO_2$, and $\Delta CO/\Delta CO_2$ observed during northerly flows were $0.0045\,\mu g C\,m^{-3}$/ppbv, $0.13\,\mu g C\,m^{-3}$/ppmv, and 49.4 ppbv/ppmv, respectively, agreeing reasonably with their respective emission ratios derived from regional emission inventories.

1 Introduction

A major portion of the fine-mode aerosols in the urban atmosphere are carbonaceous aerosols. Carbonaceous aerosols are generally classified into organic carbon (OC) and black carbon (BC). BC can absorb light, therefore acting as a positive radiative forcing agent in the troposphere and causing a negative radiative forcing at the earth surface (Ramanathan et al., 2008; Jacobson et al., 2000; Chuang et al., 2003; Kim et al., 2008). It has been estimated that the global mean clear-sky radiative forcing of BC is about +0.4–0.8 W/m^2 (IPCC, 2001). BC also causes several health effects, including allergy, respiratory, and cancer-like diseases (Jansen et al., 2005; Alessandrini et al., 2006; Sugilia et al., 2007). BC and CO are mainly produced from incomplete combustion

of fossil fuels and biomass burning; therefore, their relative emissions can be used to characterize major emission sources influencing measurement site (Hansen et al., 1989).

Emissions of various gaseous and particulate pollutants in Asia are increasing due to rapid industrialization and urban development (Streets et al., 2003). Elevated levels of the various aerosols and gaseous species in East Asian countries are of great concern because of their impacts on the atmospheric environment on regional and continental scales, for instance a reduction in precipitation of 10–20% and increasing tendency of floods and drought (Huang et al., 2007; Menon et al., 2002). In China, major economic expansion and industrialization are occurring in mega-city clusters like Beijing, Tianjin, Bohai, and the Pearl River Delta (PRD) (Shao et al., 2006). The PRD region is a densely industrialized region where emissions from a large number of petrochemical, automobile, and electronics manufacturing units are significant. Guangzhou is the main commercial and industrial city in the PRD region, with an area of $7434.4 \, \text{km}^2$ and population of over 10 million in the year 2006.

Previous studies of anthropogenic aerosols and gaseous pollutants at Guangzhou and the surrounding urban areas mostly focused on the relationships of OC and BC and their seasonal variations (Cao et al., 2003, 2004, 2007; Duan et al., 2007; Ho et al., 2006; Cheung et al., 2005), mixing states of BC (Cheng et al., 2006), and formation of sulfate and organics (Xiao et al., 2009). Some studies have also characterized aerosol chemical composition and optical properties (Andreae et al., 2008; Liu et al., 2008; Garland et al., 2008). However, none of the previous studies have reported the relationship of BC to other combustion tracers (e.g., CO, CO_2), particularly in light of their emission inventories from different sources. These relationships can be used to characterize sources and also to validate the existing emission inventories of these species. There is a need to study the diurnal variations of aerosols and gaseous species for their source attributions, by making continuous time-resolved measurements.

For the first time, we report the temporal variations of hourly averaged BC, CO, and CO_2 in the PRD region in summer in light of transient meteorological conditions and diverse emission sources. We discuss the diurnal patterns of BC, CO, CO_2 and the ratio of OC/BC as a qualitative indicator of the age of air masses. The estimated slopes of $\Delta BC/\Delta CO$, $\Delta BC/\Delta CO_2$, and $\Delta CO/\Delta CO_2$ are compared with respective emission ratios calculated from published emission inventories (Streets et al., 2003).

2　Measurement

2.1　Observation site

As a part of the Program of Regional Integrated Experiments of Air Quality over Pearl River Delta (PRIDE-PRD 2006) campaign, continuous measurements of BC, CO, and

CO_2 concentrations were made at Guangzhou between 1 July and 31 July 2006. Figure 1a shows an emission map of BC from Guangzhou and the surrounding region (21.75° N–24.25° N 112.25° E–114.75° E, 0.5°) for the year 2000 (Streets et al., 2003), while Fig. 1b shows the road network in the Guangzhou urban region. In Fig. 1a and b, a crossed circle represents the observation site, located on the 16th floor (∼50 m above ground level (a.g.l.)) of the Guangdong Provincial Environmental Monitoring Center (GPEMC) building (23.13° N, 113.26° E). Guangzhou city is surrounded by a highway and major roads including an express highway, ring road, and Dongfeng road pass through the urban region. Dongfeng is the road closest to the observation site.

2.2　Experimental

Measurements of BC or elemental carbon (EC) and OC mass concentrations in the fine mode ($PM_{2.5}$) were made using a semi-continuous EC-OC aerosol analyzer (RT 3015, Sunset Laboratory Inc., US) with one-hour time resolution, operated by the Gwangju Institute of Science and Technology (GIST), Gwangju, South Korea. The analysis of BC and OC was based on the National Institute for Occupational Safety and Health (NIOSH) thermal-optical transmittance (TOT) protocol for pyrolysis correction (Birch and Cary, 1996; Jeong et al., 2004; Kim et al., 2006). Ambient air samples were drawn through an inlet line fitted with a cyclone with a 2.5-μm particle diameter ($PM_{2.5}$) sharp cut-off size at a flow rate of 8 LPM. Then the samples were passed through a carbon-impregnated filter (CIF) multi-channel parallel-plate denuder to remove volatile organic vapors (VOCs). Samples were collected on quartz filter paper for 44 min and then heated in four stages at increasing temperatures under a helium atmosphere to quantify the carbonaceous aerosols. As the OC vaporized during temperature ramping, it was oxidized to CO_2 in the oxidizing oven. BC was oxidized to CO_2 when the temperature was stepped up to 850 °C in the oven in presence of oxygen environment. The instrument was calibrated by auto-injection of CH_4 (5% in He) as an internal standard. The detection limit of the instrument was estimated to be $0.4 \, \mu\text{gC} \, \text{m}^{-3}$ for BC, OC, or total carbon (TC), determined as three times the standard deviation (σ) of a filtered air measurement (dynamic blank) (Kim et al., 2006; Jung et al., 2009). The quartz filter was changed every 1–2 weeks based on the laser correction factor. The calibration constant used in the instrument to calculate mass concentrations of thermal OC and BC was $18.0 \, \mu\text{gC}$ (Kim et al., 2006). The measurement uncertainty of the instrument was estimated to be 5%. The detection limit and measurement uncertainty were similar to those reported by Polidori et al. (2006), Jeong et al. (2004), Kim et al. (2006), and Jung et al. (2009) for the EC-OC analyzer (Sunset Laboratory).
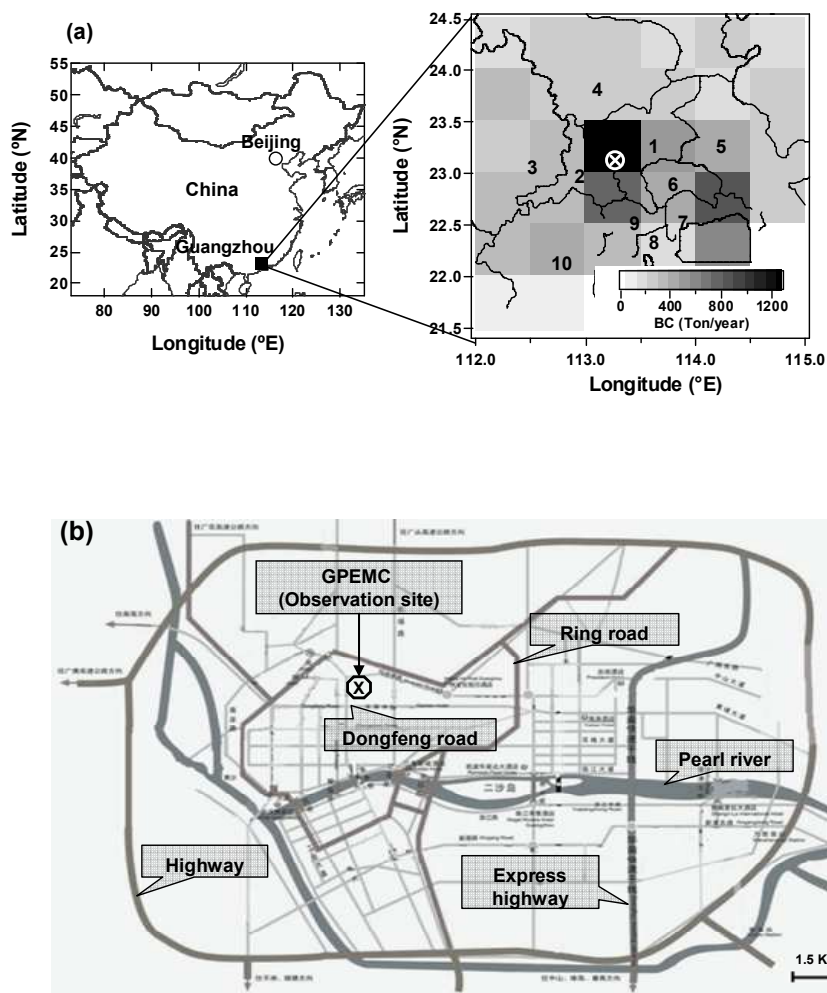
Fig. 1. (a) Spatial distribution of BC emissions (tons/year) in Guangzhou and surrounding areas (21.75° N–24.25° N, 112.25° E–114.75° E). Numeric labels are for: 1. Guangzhou, 2. Foshan, 3. Zhouqing, 4. Qianguan, 5. Huizhou, 6. Dongguan, 7. Shenzhen, 8. Zhuhai, 9. Zhongshan, and 10. Jiangmen. The white circled cross represents the observation site. **(b)** Road network surrounding the observation site in Guangzhou.

Kondo et al. (2010) compared the measurements of BC using laser incandescence (single – particle soot photometer, (SP2)), refraction (refractory mass method (RMM)), thermal-optical-transmittance (TOT), and light absorption (Continuous Soot Monitoring System (COSMOS)) methods in Tokyo. They found excellent agreement between RMM versus TOT (M_{TOT}=0.96 M_{ref}+0.11 (µgC m^{-3}), r^2=0.88) and COSMOS versus SP2 (M_{COSMOS}=0.99 M_{SP2}−0.02) (µgC m^{-3}), r^2=0.97). The good agreement between the thermal and optical methods of BC measurements has also been reported in several previous studies (Vernkatachari et al., 2006; Park et al., 2002; Sahu et al., 2009; Yang et al., 2006; Miyazaki et al., 2008). Therefore, in this study, we have used BC instead of EC throughout the manuscript.

The mixing ratio of CO was measured using a non-dispersive infrared (NDIR) absorption gas analyzer (Model 48, Thermo Environmental Instruments (TEI), US) with an integration time of one minute. CO_2 concentration was measured using an NDIR-based instrument (Model LI 7000, LI-Cor, Inc., United States) with an integration time of 10 seconds (Kondo et al., 2006; Takegawa et al., 2006). A common inlet line (Teflon tube of internal diameter (ID) ∼6 mm and length ∼10 m) was used for both analyzers from the rooftop. Because of high relative humidity levels at the measurement site in summer, air samples were passed through two sets of Nafion dryers (Perma-Pure Inc., USA) before analysis to reduce the interference of water vapor. On-site calibrations of CO and CO_2 were performed using standard mixtures with 5 ppmv of CO in air and 358 ppmv and 639 ppmv of CO_2 in air. The accuracy and precision of the CO measurements

Table 1. Relative contributions (in %) of BC, CO, and CO_2 emissions from different sources in Guangzhou urban area (21.75°–24.25 ° N, 112.25°–114.75 ° E) for the year 2000 (Streets et al., 2003).

	Domestic sector		Non-domestic sector			Total
	Fossils fuel	Biofuel	Industry	Power	Transportation	
BC	10 (2.0)	21 (4.1)	38 (7.8)	2 (0.5)	28 (5.8)	100 (20.4)
CO	3 (101.7)	10 (337.8)	47 (1624.1)	2 (66.1)	39 (1347.4)	100 (3477.2)
CO_2	5 (8140.0)	6 (10 020.6)	32 (50 481.0)	39 (61 507.4)	17 (26 540.1)	100 (156 689.1)

( ) Emissions of each species (in Gg yr $^{-1}$).

were 1.4% and 4 ppbv (at CO=400 ppbv in 1 min.), while for CO_2 these were 0.2% and 0.3 ppmv (at CO_2=400 ppmv in 10 s), respectively. Further details of these analyzers were reported by Takegawa et al. (2009).

Meteorological data were obtained from the nearest meteorological station (ZDQ-13), manufactured and operated by Sun Yet-san University, China. The accuracies of meteorological parameters like wind speed, wind direction, ambient temperature, ambient pressure, and rainfall were about $\pm 0.3 \, \mathrm{m\,s^{-1}}$, $\pm 5\,°$ (at wind speed 0.5 m s^{-1}), 0.2 °C, 0.2 hPa, and 0.4 mm h^{-1}, respectively. The Mixed Layer Height (MLH) or the depth of the Planetary Boundary Layer (PBL) was estimated from the vertical profiles of aerosol extinction coefficient at a wavelength of 1064 nm from a Light Detection and Ranging (LIDAR) system operated by the National Institute for Environmental Studies (NIES), Japan. The MLH is defined as the height where the gradient of the attenuated backscattering coefficient (ATBC) at 1064 nm is a minimum. Details of the LIDAR measurements during the PRD campaign were discussed by Sugimoto et al. (2009).

3   Emissions of BC, CO and CO_2

Figure 1a shows the spatial distribution of emissions of BC (Streets et al., 2003). Although not shown, the emissions of CO and CO_2 exhibited similar distributions in Guangzhou and the surrounding urban region. The observation site is located within the grid (0.5°×0.5°) of highest emissions of BC, while other major emission grids are distributed in the southeast (SE) corridors. These major BC emissions are mainly from the urban areas of Guangzhou, Foshan, Shenzhen, Zhongshan, and Jiangmen, in decreasing order. Apart from the emission sources in Guangzhou, the impact of anthropogenic activities in Foshan city could be significant, as it is the urban region closest to the measurement site. Foshan is the third largest manufacturing base in the PRD region, after Shenzhen and Guangzhou. Emissions from the sources located along the northwest (NW) and northeast (NE) sectors are less, compared to the contributions from the southern regions. Table 1 illustrates the emissions of BC, CO, and CO_2 from domestic and non-domestic sectors for the year 2000 (Streets et al., 2003). The domestic sector is

further sub-categorized as biofuels and fossil fuels, collectively contributing about 30% of BC and 10–15% each of CO and CO_2 to the total emissions. The non-domestic sector includes emissions from industry, power generation, and transport contributing about 70% of BC and 85–90% of CO and CO_2. Among these sources, the emissions from industry and transport mainly contribute to the non-domestic sector (Streets et al., 2003). In the Guangzhou urban region, the emissions of BC, CO, and CO_2 from biomass burning are 0.00024, 0.032, and 0.513 Gg/year, respectively; however, these fractions are not significant compared to the contributions from the other sectors given in Table 1. It is important to mention that these estimates are subject to large uncertainties, e.g., 484% for BC, 156% for CO, and 16% for CO_2 for China (Streets et al., 2003). However, there are sporadic burnings of automobile tires and house rubbish in Guangzhou and surrounding areas and emission estimates of such activities are not reported (http://www.mea-ren.org/files/upload/archive/Jan.%2015,%202010).

As suggested by previous studies (Tan et al., 2006; Bi et al., 2003; Zhou et al., 2007; Shao, 2001) and the emission inventory of Streets et al. (2003), the transport sector could be an important source of BC in Guangzhou, as it accounts for about 30% of total BC emissions (Table 1). Figure 2 illustrates the hourly averaged diurnal variations of traffic volume comprising heavy-duty (HDV), medium-duty (MDV), and light-duty vehicles (LDV) on the Dongfeng Middle Road, recorded during 18–24 July 1999, and 12–18 October 1999 (Xie et al., 2003). Since traffic data were not recoded during the present study we rely on previous data reported for Guangzhou city (Xie et al., 2003). Although these data were recorded about 7 years before the present study and can have some limitations in this context, we assume that the diurnal pattern remains nearly unchanged. The total traffic volume is lowest during early morning hours, increases after about 07:00 h, peaks between 07:00–11:00 h, and then decreases gradually until midnight. However, HDVs show a different pattern, remaining nearly stable during the day and late evening hours (Fig. 2). There was no traffic regulation in Guangzhou for entry restrictions for heavy-duty vehicles in the city area before July 2007 (http://www.chinacourt.org/flwk/show1.php?file-id=118290) as there is in Beijing to
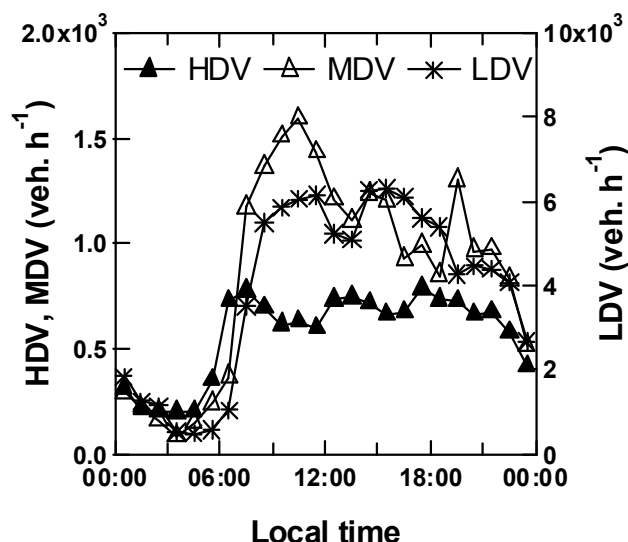
Fig. 2. Diurnal patterns of heavy-duty (HDV), medium-duty (MDV) and light-duty (LDV) vehicles on the Dongfeng middle road, recorded during 18–24 July 1999 and 12–18 October 1999 (Xie et al., 2003).

Fig. 3. Time series variations of hourly averaged concentrations of BC, CO, CO_2 and some meteorological parameters.

avoid traffic jams (Han et al., 2009). It is important to note that the emission factor of BC in HDV exhaust is significantly higher than LDV and MDV (Westerdahl et al., 2009, and references therein).

4 Temporal variations

Figure 3 shows temporal variations of hourly averaged BC, CO, CO_2, and some meteorological parameters. The average ± SD of wind speed, temperature, relative humidity, and pressure were $2.6 \pm 1 \, \text{m s}^{-1}$, $31 \pm 3 \, ^\circ\text{C}$, $76 \pm 14\%$, and 1003 ± 5 hPa, respectively, during the campaign. Meteorological conditions were fairly stable, with steady wind flow ($\sim$3 m s^{-1}) from the South China Sea during 2–11 July. The concentrations of BC remained constant at $\sim$4 μgC m^{-3} for this period, except for two episodes of elevated levels in the early morning of 3 July and evening of 7 July. Observations during 12–13 July were impacted by rather weak northerly flow ($<$2 m s^{-1}). These stagnant weather conditions could have favored the accumulation of pollutants, resulting in higher BC and CO of $\sim$12.5 μgC m^{-3} and $\sim$1700 ppbv, respectively. A typhoon (named Billis) originating over the southern oceanic region hit the PRD on 15 July and continued until 17 July. Significant amounts of these species were likely scavenged by the rain associated with the strong wind flow during the typhoon circulation (Fig. 3). Relatively lower concentrations of pollutants were observed until 18 July due to dilution caused by the mixing of cleaner air. No significant changes in the concentrations of BC or CO were observed during 19–22 July. Later, during 23–26 July, observa-

tions were influenced by stagnant weather, and consequently BC and CO reached levels of 15.0 μgCm^{-3} and 2500 ppbv, respectively, on some occasions. Another typhoon event, named Kaemi, arrived over the PRD with strong winds and rain during 27–28 July. The long-term trend of CO_2 mixing ratio was similar to that of BC and CO. To avoid any bias, measurements conducted during the episodes of rainfall have been excluded from the statistical and correlation analyses.

Generally, the concentrations of BC, CO, and CO_2 appear to have been influenced by changes in meteorological conditions. To investigate the impact of long-range transport of the air masses, 3 – day isobaric back trajectories were calculated twice per day (at 00:00 local time (LT) and 14:00 LT) using the Hybrid Single Particle Lagrangian Integrated Trajectory (HYSPLIT-4) model (Draxler and Rolph, 2003). Figure 4 shows the back trajectories (once per day), each trajectory starts at 00:00 LT and 50 m a.g.l. at the measurement site. The pattern of trajectories at noon was almost as same as that analyzed for midnight; therefore, the latter are not been shown in Fig. 4. Based on the trajectory analyses of the entire period of observations, the air masses at the Guangzhou site have been classified into two main categories depending on the direction of transport, from northerly (red lines in Fig. 4) and southerly (blue lines in Fig. 4) directions. Air masses categorized as northerly air (about 25% of the measurements,) arrived mostly from northwest (NW) direction and prevailed during 12–14 July and 23–26 July. However, the flow of northerly air masses was rather stagnant, as the trajectories circulated mostly within the PRD region. Therefore, the measurements of northerly air represent
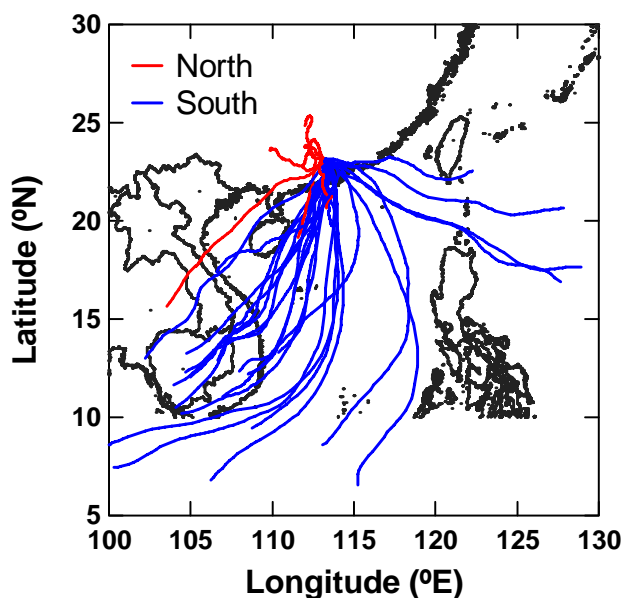
Fig. 4. Three-day back trajectories each started at 00:00 h from the observation site (23.13° N, 113.26° E, and 50 m a.g.l.). The trajectories were calculated using HYSPLIT-4 model (NOAA/ARL, FNL meteorological archived dataset).

the influence of emissions from various sources in the PRD. The southerly air masses originated over the South China Sea and prevailed during 1–11 July, 16–22 July, and 27–31 July, influencing ∼75% of the entire campaign. The southerly flow resulted in significant dilution of primary pollutants and hence represents the observations of fresh emissions from local sources in Guangzhou.

Data measured in both northerly and southerly air masses are further classified into two categories, day (08:00–18:00 h) and night (20:00–06:00 h). We have excluded the data measured during 07:00–08:00 h and 19:00–20:00 h to avoid any biases on the measurements caused by the rapid changes in meteorological parameters. The daytime measurements represent observations of well-mixed air due to both higher boundary layer depth and wind speed. Statistics of BC, CO, and CO_2 measured in different categories of air masses are presented in Table 2. The errors in the measurements are assumed to be normally distributed. Hence, in this manuscript, we have expressed the variability observed in the concentrations of the species with ±standard deviation (SD or $\pm 1\sigma$, within a confidence interval of 68.2%). The average (day + night) mass concentrations of BC and mixing ratio of CO in the northerly air masses were 6.3 µgC m^{-3} and 1059 ppbv, while these were 4.3 µgC m^{-3} and 693 ppbv in the southerly air masses, respectively. In the northerly air, the average levels of BC and CO were about 30% higher than those measured in the southerly air. Based on all measured data, the average concentrations of BC, CO, and CO_2 were 4.7 µgC m^{-3}, 798 ppbv, and 400 ppmv, respectively.

During northerly flow, the meteorological conditions favored stagnation, causing higher levels of pollutants in ambient air. In contrast, southerly air masses were generally dominated by cleaner marine air from the South China Sea (Liu et al., 2008; Lai et al., 2007; Yeung et al., 2006). We have estimated the background concentrations, illustrated in Table 3. The background concentration is defined as the 1.25 percentile of the dataset (Kondo et al., 2006). The background concentrations of both BC and CO in the northerly air masses were higher by abouta factor of two than those estimated for southerly air masses.

5 Diurnal variations

The diurnal plots of the hourly average ± SD of BC, CO, CO_2, wind speed, MLH, and OC/BC ratio for both northerly and southerly air masses are shown in Fig. 5. The concentrations of BC, CO, and CO_2 started increasing from the early morning hours (05:00–06:00 h). BC, CO, and CO_2 attained their peaks at around 07:00–09:00 h. As the day advances, the levels of BC, CO, and CO_2 decrease gradually during the afternoon (13:00–15:00 h) due to higher vertical mixing caused by a simultaneous increase in wind speed and MLH. In the evening hours, concentrations of BC, CO, and CO_2 exhibit increasing trends and peaks at around 19:00–21:00 h. The peaks of BC, CO, and CO_2 concentrations coincide with rush hours, and therefore can be attributed mainly to traffic emissions. Similar features have been reported from measurements in other urban regions (Glasius et al., 2006; Park et al., 2005; Latha et al., 2004; Baumgardner et al., 2007; Dutkiewicz et al., 2009; Cao et al., 2009). OC/BC ratios of ∼1.0–2.0 µgC m^{-3}/µgC m^{-3} are often associated with fresh emissions from primary sources (Turpin and Huntzicker 1991, 1995; Lin et al., 2009). As can be seen in Fig. 5, the peaks in the concentrations of BC, CO, and CO_2 coincided with the lower values of the OC/BC ratio, suggesting the influence of fresh emissions mainly from traffic. During the southerly flow, the low OC/BC ratios of ∼1.0 µgC m^{-3}/µgC m^{-3} during morning peak hours can be attributed to major emissions from traffic (Fig. 2). On the other hand, the higher OC/BC ratios of ∼2.0 µgC m^{-3}/µgC m^{-3} during the morning rush hours of northerly flow could be due to the emissions from various sources in the PRD and also due to photochemical ageing to some extent.

In northerly air the diurnal variations of BC, CO, and CO_2 were more pronounced than those in southerly air. This comparison is consistent with the variations in the meteorological parameters, for example, MLH and wind speed show stronger variation in northerly air (see Fig. 5). In southerly air, although the diurnal variations of meteorological parameters were less pronounced compared to northerly air, the daytime concentrations of BC and CO do not show any clear dependencies on local time. The effect of dilution seems

Table 2. Statistics of BC, CO, and CO_2 observed in different categories at Guangzhou. The daytime and nighttime hours were 08:00–18:00 h and 20:00–06:00 h, respectively. To avoid any bias due to the transition phase of wind speed and MLH, the data measured during 07:00–08:00 h in the morning and 19:00–20:00 h in the evening were removed from the analysis.

		BC (μgC m^{-3})				CO (ppbv)				CO_2 (ppmv)			
		Min.	Max.	Average±SD	Median	Min.	Max.	Average±SD	Median	Min.	Max.	Average±SD	Median
North	Day	2.7	12.9	5.8±2.4	5.2	429	2282	1025±441	909	383	452	402±14	400
	Night	3.9	18.7	6.8±2.5	6.3	443	3107	1092±737	803	383	446	410±14	408
South	Day	1.2	9.7	4.1±1.4	3.8	315	2729	734±315	688	373	436	396±11	395
	Night	1.1	17.0	4.4±2.4	3.8	263	1991	652±338	556	380	452	397±10	395
All data		1.1	18.7	4.7±2.3	4.2	202	3162	798±459	685	373	453	400±13	398
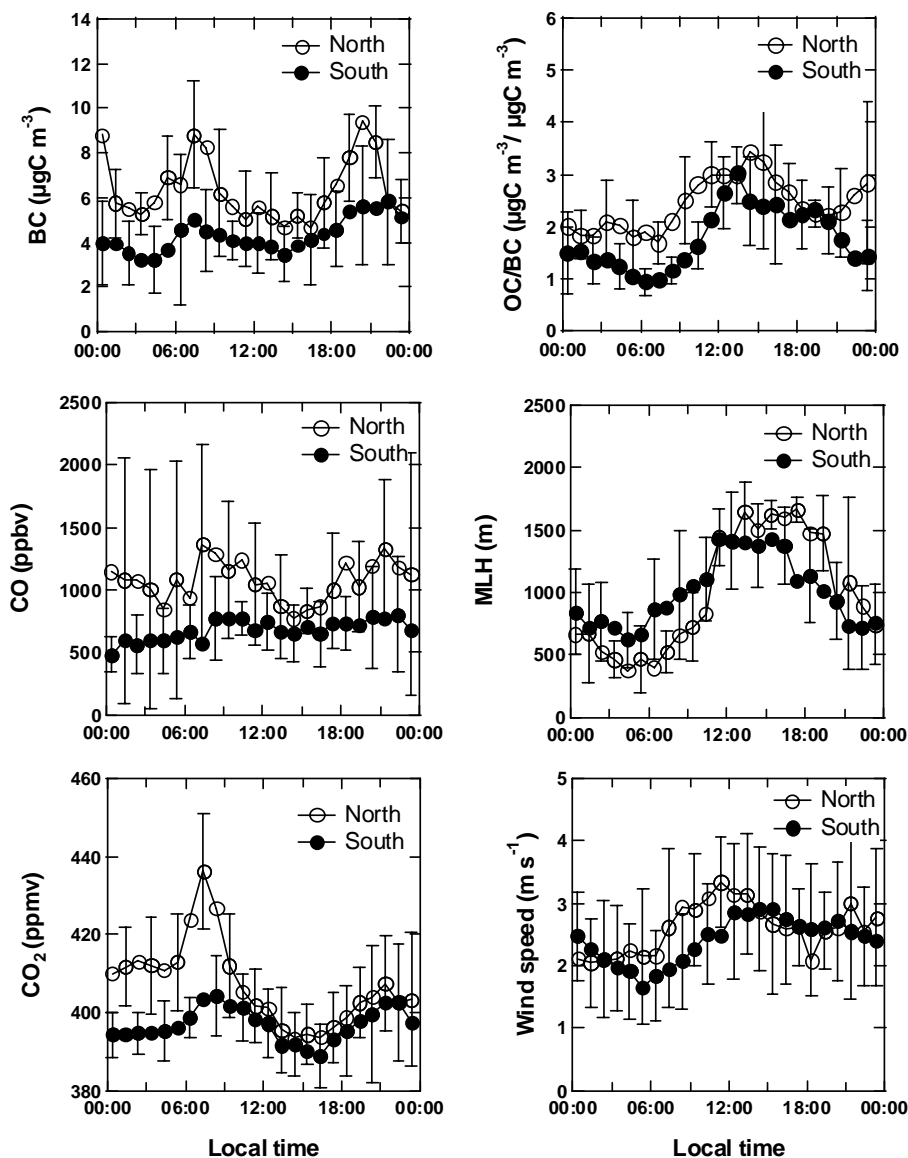
Fig. 5. Diurnal variations of hourly average±SD of BC, CO, CO_2, wind speed, mixed layer height (MLH), and the ratios of OC/BC in northerly and northerly air masses.

Table 3. Background concentrations (1.25 percentiles) of BC, CO, and CO_2.

		BC (μgC m^{-3})	CO (ppbv)	CO_2(ppmv)
North	Day	2.79	430	383
	Night	3.88	448	386
South	Day	2.33	333	376
	Night	1.26	295	383
All data		1.27	322	379

Fig. 6. Diurnal variations of hourly BC and heavy-duty vehicles (HDV) in Guangzhou. The traffic volume of HDV is an hourly average, recorded during 18–24 July 1999, and 12–18 October 1999 on the Dongfeng middle road, (Xie et al., 2003).

to be counterbalanced due to the strong daytime emission sources near the observation site. The diurnal trend of BC in southerly flow closely follows the pattern of HDV traffic, suggesting their major influence during the daytime (Fig. 6). The combustion of diesel fuel in these vehicles is an important source of BC (Bond et al., 2004). The transport of BC from the strong daytime emission sources situated in the south of Guangzhou could have counterbalanced the dilution caused by higher wind and MLH (http://www.idsgroup.com/profile/pdf/industry_series/LFIndustrial2.pdf). It would be interesting to study the "weekend effect" in the concentrations of primary pollutants; however, the number of weekend days were limited in the present observations. Thus, a conclusive remark about the impact of weekend reductions in anthropogenic activities on the diurnal variations of these species is not possible.

6 Dependence of BC on wind speed and MLH

Apart from the local time dependence of the emissions, variations in meteorological parameters can influence the concentrations of pollutants; however, their contributions cannot be separated in a strict sense. Figure 7 shows scatter plots of BC with wind speed and MLH and also coded for the local time of the measurements. A small dependency of BC on wind speed was observed in both northerly and southerly air masses. On the other hand, dependencies of BC on MLH were not observed during the flows of both northerly and southerly air masses. Overall, the dependencies of BC on wind speed and MLH seem to be independent of the time of the measurements. The relationship of BC to MLH explains that the levels of BC could have been influenced by strong daytime emissions. The presence of stable aerosol layers above the boundary layer could have also inhibited the dilution of BC due to increasing MLH (Sugimoto et al., 2009)
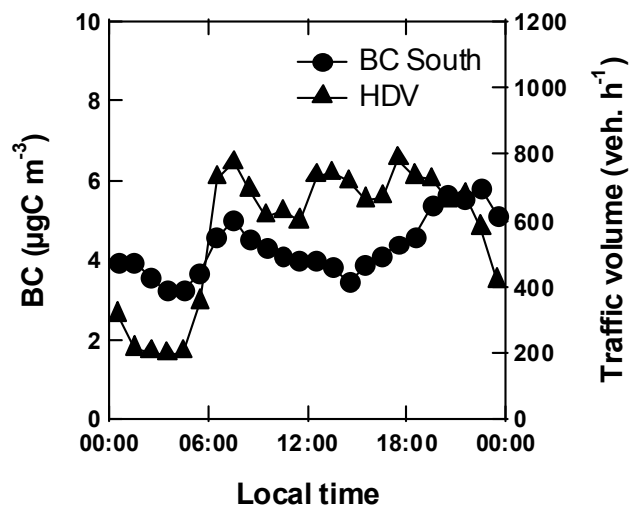
7 Relationships

7.1 BC with CO and CO_2

The relationships of BC to CO and CO_2 can be useful in investigating the transport of BC from source regions. For example, ΔCO/ΔCO_2 ratios have been used to identify the origin of air masses (Takegawa et al., 2004). Estimates of the transport efficiency of BC from source region to the boundary layer and from the boundary layer to the free troposphere have been based on BC/CO correlation slopes and emission ratios calculated from emission inventories (Park et al., 2005; Sahu et al., 2008). Figure 8 shows scatter plots of the pairs BC-CO, BC-CO_2, and CO-CO_2 using all data. Slopes were calculated using a bi-variable linear fit regression method. The uncertainties of slopes were determined as $\pm 2\sigma$ (within 95.4% confidence interval). Table 4 illustrates details of the linear fit regression slopes of ΔBC/ΔCO, ΔBC/ΔCO_2, and ΔCO/ΔCO_2. The slopes of ΔBC/ΔCO and ΔBC/ΔCO_2 of daytime data are lower than those at nighttime in both types of air masses, whereas ΔCO/ΔCO_2 shows the opposite pattern (Table 4). Reliable ΔBC/ΔCO slopes are useful for assessing long-range transport of BC with reference to CO. The linear fit regression slopes of ΔBC/ΔCO, ΔBC/ΔCO_2, and ΔCO/ΔCO_2 over the whole dataset are 0.0054 μgC m^{-3}/ppbv, 0.14 μgC m^{-3}/ppmv, and 46.4 ppbv/ppmv, respectively. Overall, the moderate correlations between BC-CO, BC-CO_2, and CO-CO_2 are expected at the observation site in Guangzhou, where measurements were influenced by the emissions from various sources.

Table 4. Observed BC-CO, BC-CO$_2$, and CO-CO$_2$ linear regressions slopes ($\pm 2\sigma$, within 95.4% confidence interval).

		$\Delta BC/\Delta CO$ ($\mu gC\,m^{-3}$/ppbv)		$\Delta BC/\Delta CO_2$ ($\mu gC\,m^{-3}$/ppmv)		$\Delta CO/\Delta CO_2$ (ppbv/ppmv)	
		Slope	r^2	Slope	r^2	Slope	r^2
North	Day	0.0045±0.0008	0.68	0.13±0.02	0.62	49.4±6.2	0.60
	Night	0.0069±0.0016	0.58	NA	–	NA	–
South	Day	0.0051±0.0010	0.59	0.12±0.02	0.55	57.4±3.8	0.46
	Night	0.0070±0.0008	0.75	0.21±0.02	0.76	34.9±3.0	0.67
All data	Day	0.0045±0.0010	0.51	0.13±0.02	0.57	53.2±3.8	0.50
	Night	0.0067±0.0008	0.72	0.16±0.02	0.55	NA	–
All data		0.0054±0.0004	0.61	0.14±0.02	0.58	46.4±3.0	0.45

NA: not available.
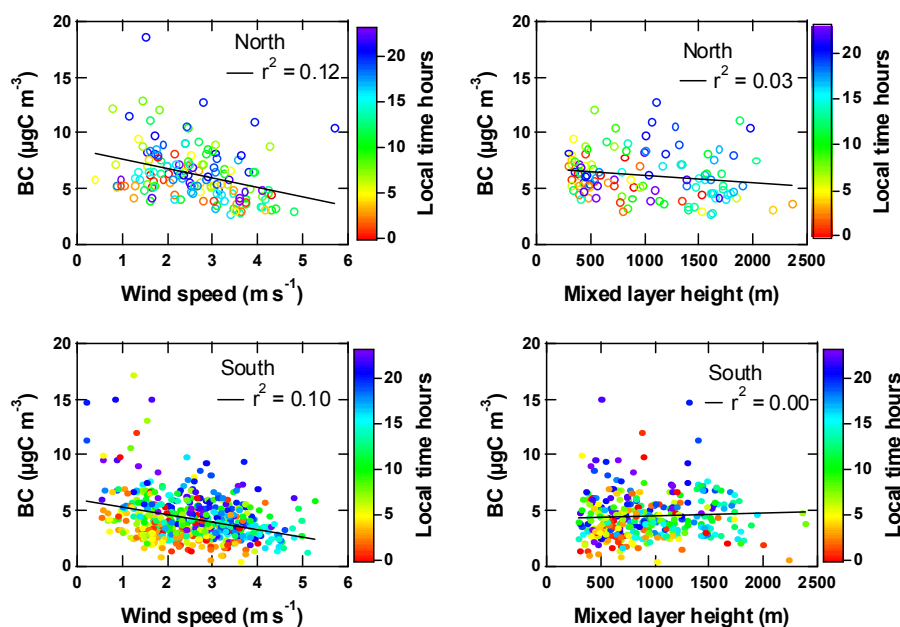
Fig. 7. Scatter plots of BC with wind speed and MLH. Northerly and southerly air masses are represented by open and closed circles, respectively. The vertical color bar represents the local time of measurements of BC.

8 Comparisons

8.1 Guangzhou and Beijing

Guangzhou and Beijing are two major urban regions of China where vehicular emissions can be an important source of ambient BC (Streets et al., 2003). In this study, we have compared the diurnal relations of BC in southerly flows with the traffic of heavy-duty vehicles in both cities (see Fig. 9). Similar to our observations, the diurnal variation of BC follows the traffic of heavy-duty diesel trucks (HDDTs) in Beijing (Han et al., 2009). In Beijing, the concentration of BC shows a diurnal cycle opposite to that observed in Guangzhou, as it was observed to be higher (lower) during the night (day). Similarly, the traffic volume shows this opposite diurnal pat-

tern in these cities. Kondo et al. (2006) also report a close relationship of ambient BC with traffic in Tokyo. The present and previous studies in urban regions suggest that the concentrations of ambient BC are mainly controlled by the emissions from heavy duty-vehicles.

8.2 Previous observations

For the first time we report hourly time-resolved measurements of BC at Guangzhou. Here we compare the average BC of northerly flows of the present study with previous measurements conducted at different sites in Guangzhou during the summer (Fig. 10). The BC concentration of $6.2\,\mu gC\,m^{-3}$ in northerly flows of this study agrees well with the average of $6.0\,\mu gC\,m^{-3}$ (range $4.6–7.9\,\mu gC\,m^{-3}$) of all other
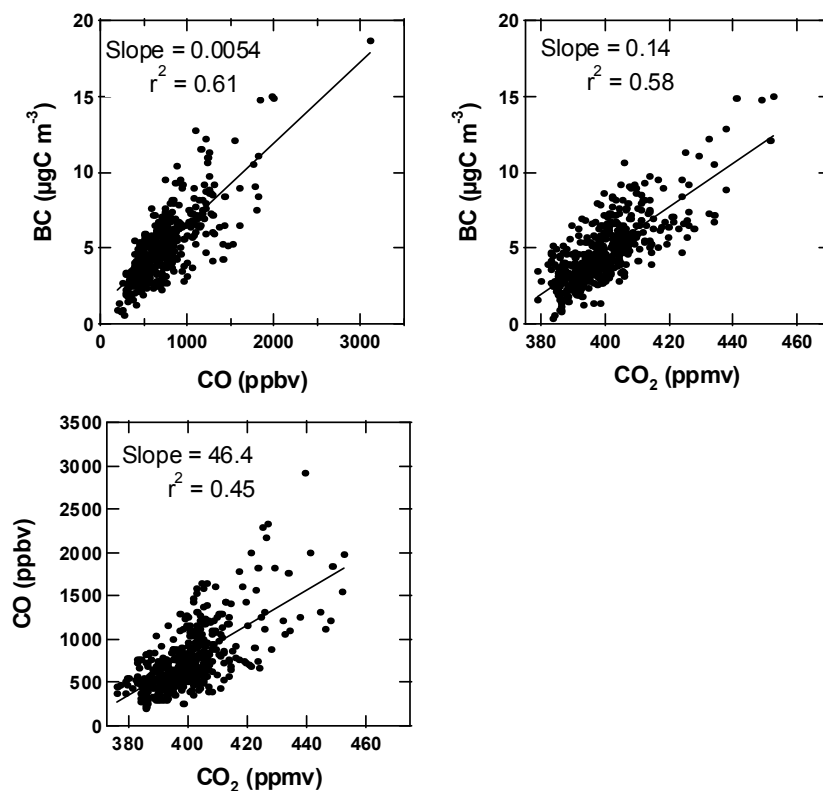
Fig. 8. Scatter plots of BC-CO, BC-CO_2, and CO-CO_2 in all dataset measured during the campaign.
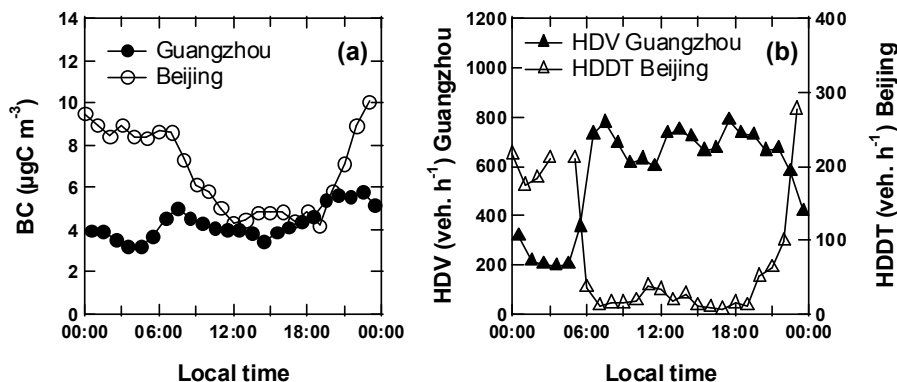
Fig. 9. Diurnal variations of **(a)** BC and **(b)** heavy-duty vehicles (HDV) in Guangzhou and heavy-duty diesel trucks (HDDT) in Beijing. The traffic volume of HDV includes buses and trucks, while HDDT is heavy-duty diesel trucks.

sites in Guangzhou (Fig. 10), situated at Zhongshan University (8 km from GPEMC), Liwan (5 km), Wushan (19 km), Huangpu (~17 km), and Longgui (~28 km) (Duan et al., 2007; Cao et al., 2003, 2004). Hence the average BC of northerly flows represents the level of BC emissions in the PRD region.

A comparison of observed BC and $\Delta BC/\Delta CO$ with that reported for other major urban regions of Asia is shown in Table 5. The BC mass concentration and slopes of

$\Delta BC/\Delta CO$ at Guangzhou are comparable to those observed in Beijing (China), Gwanju (South Korea), Hyderabad (India), Karachi (Pakistan), and Tokyo (Japan). These results are expected, as traffic emissions are an important source of BC and CO in these urban regions. The values of $\Delta BC/\Delta CO_2$ and $\Delta CO/\Delta CO_2$ at Guangzhou (Table 4) agree reasonably with 0.12–0.19 μgC m^{-3}/ppmv and 30.2–43.9 ppbv/ppmv, respectively, in Beijing (Han et al., 2009).

Table 5. Concentrations of BC aerosol and linear fit regression slopes measured in major urban regions of Asia.

Location and measurement period	BC (μgC m^{-3})	$\Delta BC/\Delta CO$ (μgC m^{-3}/ppbv)	Method of BC analysis	References
Guangzhou, China (Jul 2006)	4.7	0.0054	TOT	Present study
Guangzhou, China (Oct–Nov 2004)	7.1	0.0079	TOT	Andreae et al. (2008)
Beijing, China (2005–2006)	6.9	0.0035–0.0058	TOT	Han et al.(2009)
Tokyo, Japan (2003–2005)	1.9	0.0057	TOT	Kondo et al. (2006)
Gwanju, South Korea (Mar–May 2001)	5.7	0.0060	TOT	Park et al. (2005)
Hyderabad, India (Jan 2004)	1.5–11.2	0.0073	L. Abs.	Latha et al. (2004)
Karachi, Pakistan (2006–2007)	5.9	NA	L. Abs.	Dutkiewicz et al. (2009)

NA: not available;
TOT: thermal-optical-transmittance;
L Abs.: Light absorption.

Table 6. BC/CO (μgC m^{-3}/ppbv), BC/CO$_2$ (μgC m^{-3}/ppmv), and CO/CO$_2$ (ppbv/ppmv) emission ratios derived from emission factors (grams of pollutant evolved per kilogram of fuel burned).

| | Transport | | Industry | Domestic | | Biomass burning |
	Diesel[d,e,g,h]	Gasoline[d,h]	Coal[d]	Coal[d,f]	biofuels[c,d]	(crop residue)[a,b,c]
BC/CO	0.0013–0.055	0.0031–0.0115	0.0017–0.0182	0.0019–0.0572	0.0087–0.0266	0.0056–0.016
BC/CO$_2$	0.15	0.06–0.11	0.04–0.74	0.11–3.56	0.69–1.75	0.53–1.10
CO/CO$_2$	8.6–65.2	33.5	23.5–40.4	53.3–62.2	52.9–98.5	45.7–123.6

[a] Dhammapala et al. (2007), [b] Cao et al. (2008), [c] Andreae and Merlet (2001), [d] Streets et al. (2003), [e] Dickerson et al. (2002), [f] Boucher et al. (2008), [g] Sanchez et al. (2009), [h] Westerdahl et al. (2009).

8.3 Correlation slopes and emission ratios

To understand the importance of major emission sources impacting the levels of BC, CO, and CO$_2$ in the Guangzhou urban region, the slopes of $\Delta BC/\Delta CO$, $\Delta BC/\Delta CO_2$, and $\Delta CO/\Delta CO_2$ are compared with the emission ratios derived from emission factors reported for different sources (Table 6). In Table 6 ranges of emission ratios of BC-CO, BC-CO$_2$, and CO-CO$_2$ are presented for different sectors. Although we have seen significant differences in the diurnal variations of the concentrations of primary pollutants depending on the flows from northerly and southerly directions, however, the slopes of $\Delta BC/\Delta CO$, $\Delta BC/\Delta CO_2$ and $\Delta CO/\Delta CO_2$ do not vary significantly in both types of air masses. As the measurements of northern air can represent the regional-scale emissions in the PRD, here we have compared the observed $\Delta BC/\Delta CO$, $\Delta BC/\Delta CO_2$, and $\Delta CO/\Delta CO_2$ of northerly air masses with the emission ratios derived from fuel-based emissions factors (Table 6). The observed slopes of $\Delta BC/\Delta CO$ (0.0045 μgC m^{-3}/ppbv), $\Delta BC/\Delta CO_2$ (0.13 μgC m^{-3}/ppmv), and $\Delta CO/\Delta CO_2$ (49.4 ppbv/ppmv) in northerly air masses are within the ranges of emissions ratios estimated for diesel, gasoline and coal from transport, industry, and domestic sectors (Table 6). However, emissions from other sectors may influence the observations of these slopes.

Comparison of observed slopes of $\Delta BC/\Delta CO$, $\Delta BC/\Delta CO_2$, and $\Delta CO/\Delta CO_2$ with their emission ratios derived from the inventories can be useful to validate the inventory data. Table 7 shows sector-wise emission ratios of BC/CO, BC/CO$_2$, and CO/CO$_2$ for the urban regions of Guangzhou using the Streets et al. (2003) inventory data for the year 2000. The slopes of $\Delta BC/\Delta CO$ (0.0045 μgC m^{-3}/ppbv), $\Delta BC/\Delta CO_2$ (0.13 μgC m^{-3}/ppbv), and $\Delta CO/\Delta CO_2$ (49.4 ppbv/ppmv) observed in the northerly air masses are comparable to the emission ratios of BC/CO, BC/CO$_2$, and CO/CO$_2$, respectively, derived for both industrial and transport sectors. The emissions from these two sectors collectively contribute about 70% of BC, 85% of CO, and 50% CO$_2$ to the total emissions of these species (Table 1). Thus, the slopes observed in this study tend to validate the emission inventories of BC, CO, and CO$_2$ from the transport and industrial sectors. However, this conclusion may have limitations mainly due to the limited period of observations in the present study and also due to significant uncertainties in the inventory estimates. The BC-CO, BC-CO$_2$, and CO-CO$_2$ emission ratios of Guangzhou are agreed reasonably with those of Beijing reported by Han et al. (2009).

Table 7. Emission ratios of BC/CO (μgC m^{-3}/ppbv), BC/CO$_2$ (μgC m^{-3}/ppmv), and CO/CO$_2$ (ppbv/ppmv) derived from the inventory of Streets et al. (2003). Comparison of the emission ratios of Guangzhou to those of Beijing derived from the total emissions using the same inventory data.

	Domestic sector		Non-domestic sector			Guangzhou Total	Beijing[a]
	Fossils fuel	Biofuel	Industry	Power	Transportation		
BC/CO	0.0225	0.0139	0.0055	0.0087	0.0049	0.0067	0.0050
BC/CO$_2$	0.44	0.74	0.28	0.01	0.39	0.23	0.24
CO/CO$_2$	19.6	53.0	50.5	1.7	79.8	34.9	47.6

[a] Values taken from Han et al. (2009).
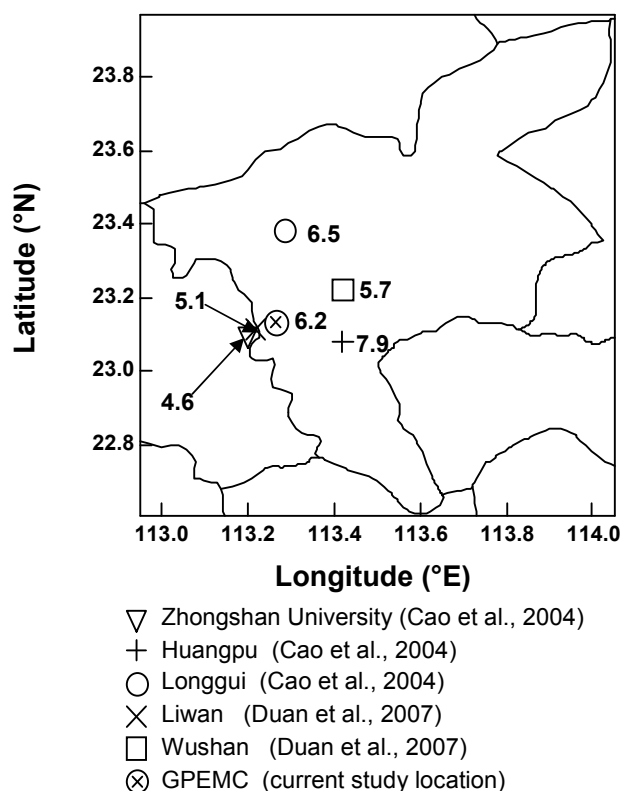
Fig. 10. Comparison of the average BC observed during northerly flows with previous measurements conducted at different sites in Guangzhou in the summer season.

9   Conclusion

As part of the PRIDE-PRD 2006 campaign, measurements of mass concentrations of BC and mixing ratios of CO and CO$_2$ were conducted at an urban site in Guangzhou, China during July 2006. Major emissions of BC in Guangzhou are from industry, transport, biofuels, and fossils fuels. The average concentrations of BC, CO, and CO$_2$ were 4.7 μgC m^{-3}, 798 ppbv and 400 ppmv, respectively, during the campaign. Trends in BC, CO, and CO$_2$ concentrations were influenced by local meteorology. Trajectory analysis suggests that the observations in northerly air masses represent the emissions from the PRD region, while southerly air masses from the South China Sea tend to dilute the ambient air concentrations of pollutants in Guangzhou. Consequently, the background concentration of BC in northerly air masses was higher by about a factor of two to those determined for southerly flow. The diurnal patterns of BC, CO, and CO$_2$ exhibited primary peaks during the morning and secondary peaks in the evening hours coinciding with rush-hour traffic. The ratios of OC/BC were lower during the morning rush hours, suggesting the dominance of fresh emissions. The diurnal variations of BC, CO, CO$_2$ were stronger in the northerly air masses than those observed in southerly flow. The diurnal patterns of BC measured during the southerly flow closely follow the patterns of HDV traffic, suggesting their major influence in the variation of primary pollutants. The average concentration of BC measured during the northerly flow agrees well with previous measurements conducted at different sites in Guangzhou and hence represent the regional-scale emissions of BC in the PRD. The slopes of ΔBC/ΔCO (0.0045 μgC m^{-3}/ppbv), ΔBC/ΔCO$_2$ (0.13 μgC m^{-3}/ppmv) and ΔCO/ΔCO$_2$ (49.4 ppbv/ppmv) observed in northerly air masses agree reasonably with the respective emission ratios.

References

Andreae, M. O. and Metlet, P.: Emission of trace gases and aerosols from biomass burning, Global Biochem. Cy., 15(4) 955–966, 2001.

Andreae, M. O., Schmid, O., Yang, H., Chanda, D., Yu, J. Z., Zeng, L. M., and Zhang, Y. H.: Optical properties and chemical composition of the atmospheric aerosol in urban Guangzhou, China, Atmos. Environ., 42, 6335–6350, 2008.

Alessandrini, F., Schulz, H., Takenaka, S., Lentner, B., Karg, E., Behrendt, H., and Jakob, T.: Effects of ultrafine carbon particle inhalation on allergic inflammation of the lung, J. Allerg. Clinic. Immunolo., 117(4), 824–830, 2006.

Baumgardner, D., Kok, G. L., and Raga, G. B.: On the diurnal variability of particle properties related to light absorbing carbon in Mexico City, Atmos. Chem. Phys., 7, 2517–2526, doi:10.5194/acp-7-2517-2007, 2007.

Bi, X., Sheng, G., Peng, P., Chen, Y., Zhang, Z., and Fu, J.: Distribution of particulate- and vapor-phase n-alkanes and polycyclic aromatic hydrocarbons in urban atmosphere of Guangzhou, China, Atmos. Environ., 37, 289–298, 2003.

Birch, M. E. and Cary, R. A.: Elemental carbon-based method for monitoring occupational exposures to particulate diesel exhaust, Aerosol Sci. Technol., 25, 221–241, 1996.

Bond, T. C., Streets, D. G., Yarber, K. F., Nelson, S. M., Woo, J. H., and Klimont, Z.: A technology-based global inventory of black and organic carbon emissions from combustion, J. Geophys. Res. 109, D14203, doi:10.1029/2003JD003697, 2004.

Boucher, O. and Reddy, M. S.: Climate trade-off between black carbon and carbon dioxide emissions, Energy Policy, 36, 193–200, doi:10.1016/j.enpol.2007.08.039, 2008.

Cao, J. J., Lee, S. C., Ho, K. F., Zhang, X. Y., Zou, S. C., Fung, K., Chow, J. C., and Watson, J. G.: Characteristics of carbonaceous aerosol in Pearl River Delta Region, China during 2001 winter period, Atmos. Environ., 37, 1451–1460, 2003.

Cao, J. J., Lee, S. C., Ho, K. F., Zou, S. C., Fung, K., Lib, Y., Watson, J. G., and Chow, J. C.: Spatial and seasonal variations of atmospheric organic carbon and elemental carbon in Pearl River Delta Region, China, Atmos. Environ., 38, 4447–4456, 2004.

Cao, J. J., Lee, S. C., Chow, J. C., Watson, J. G., Ho, K. F., Zhang, R. J., Jin, Z. D., Shen, Z. X., Chen, G. C., Kang, Y. M., Zou, S. C., Zhang, L. Z., Qi, S. H., Dai, M. H., Cheng, Y., and Hu, K.: Spatial and seasonal distributions of carbonaceous aerosols over China, J. Geophys. Res., 112, D22S11, doi:10.1029/2006JD008205, 2007.

Cao, J. J., Zhu, C. S., Chow, J. C., Watson, J. G., Han, Y. M., Wang, G. H., Shen, Z. X., and An, Z. S.,: Black carbon relationships with emissions and meteorology in Xi'an, China, Atmos. Res., 94, 194–202, 2009.

Cao, G., Zhang, X., Gong, S., and Zheng, F.: Investigation on emission factors of particulate matter and gaseous pollutants from crop residue burning, J. Environ. Sc. 20, 50–55, 2007.

Cheung, H. C., Wang, T., Baumann, K., and Guo, H.: Influence of regional pollution outflow on the concentrations of fine particulate matter and visibility in the coastal area of southern China, Atmos. Environ., 39, 6463–6474, 2005.

Cheng, Y. F., Eichler H., Wiedensoler, A., Heintzenberg, J., Zhang, Y. H., Hu, M., Herrmann H., Zeng, L. M., Liu, S., Gnauk, T., Bruggermann, E., and He, L. Y.: Mixing state of elemental carbon and non-light-absorbing aerosol components derived from in situ particle optical properties at Xinken in Pearl River Delta of China, J. Geophys. Res., 111, D20204, doi:10.1029/2005JD006929, 2006.

Chuang, P. Y., Duvall, R. M., Bae, M. S., Jefferson, A., Schauer, J. J., Yang, H., Yu, J. Z., and Kim, J.: Observations of elemental carbon and absorption during ACE-Asia and implications for aerosol radiative properties and climate forcing, J. Geophys. Res., 108(D23), 8634, doi:10.1029/2002JD003254, 2003.

Dhammapala, R., Claiborn, C., Simpson, C., and Jimenez, J.: Emission factors from wheat and Kentucky bluegrass stubble burning: Comparison of field and simulated burn experiments, Atmos. Environ., 41, 1512–1520, doi:10.1016/j.atmosenv.2006.10.008, 2007.

Dickerson, R. R., Andreae, M. O., Campos, T., Mayol-Bracero, O. L., Neuseuss, C., and Streets, D. G.: Analysis of black carbon and carbon monoxide observed over the Indian Ocean: Implications for emissions and photochemistry, J. Geophys. Res., 107(D19), 8017, doi:10.1029/2001JD000501, 2002.

Draxler, R. R. and Rolph, G. D.: HYSPLIT (HYbrid Single-Particle Lagrangian Integrated Trajectory) Model access via NOAA ARL READY, Website (http://www.arl.noaa.gov/ready/hysplit4.html), NOAA Air Resources Laboratory, Silver Spring, MD, 2003.

Duan, J., Tan, J., Cheng, D., Bi, X., Deng, W., Sheng, G., Fu, J., and Wong, M. H.: Sources and characteristics of carbonaceous aerosol in two largest cities in Pearl River Delta Region, China, Atmos. Environ., 41, 2895–2903, 2007.

Dutkiewicz, V. A., Alvi, S., Ghauri, B. M., Choudhary, M. I., and Husain, L.: Black carbon aerosols in urban air in South Asia, Atmos. Environ., 43, 1737–1744, doi:10.1016/j.atmosenv.2008.12.043, 2009.

Garland, R. M., Yang, H., Schmid, O., Rose, D., Nowak, A., Achtert, P., Wiedensohler, A., Takegawa, N., Kita, K., Miyazaki, Y., Kondo, Y., Hu, M., Shao, M., Zeng, L. M., Zhang, Y. H., Andreae, M. O., and Pöschl, U.: Aerosol optical properties in a rural environment near the mega-city Guangzhou, China: implications for regional air pollution, radiative forcing and remote sensing, Atmos. Chem. Phys., 8, 5161–5186, doi:10.5194/acp-8-5161-2008, 2008.

Glasiusa, M., Ketzel, M., Wahlin, P., Jensen, B., Mønster, J., Berkowicz, R., and Palmgren, F.: Impact of wood combustion on particle levels in a residential area in Denmark, Atmos. Environ., 40, 7115–7124, 2006.

Han, S., Kondo, Y., Takegawa, N., Miyazaki, Y., Oshima, N., Hu, M., Lin, P., Deng, Z., Zhao, Y., and Sugimoto, N.: Temporal variation of elemental carbon in Beijing, J. Geophys. Res., 114, D23202, doi:10.1029/2009JD012027, 2009.

Hansen, A. D. A., Convey, T. J., Steele, L. P., Bodhaine, B. A., Thoning, K. W., Tans, P., and Novakov, T.: Correlations among combustion effluent species at Barrow, Alaska: Aerosol black carbon, carbon dioxide, and methane, J. Atmos. Chem., 9, 283–299, 1989.

Ho, K. F., Lee, S. C., Cao, J. J., Li, Y. S., Chow, J. C., Watson, J. G., and Fung, K.: Variability of organic and elemental carbon, water soluble organic carbon, and isotopes in Hong Kong, Atmos. Chem. Phys., 6, 4569–4576, doi:10.5194/acp-6-4569-2006, 2006.

Huang, Y., Chameides, W. L., and Dickinson, R. E.: Direct and indirect effects of anthropogenic aerosols on regional precipitation over east Asia, J. Geophys. Res., 112, D03212,

doi:10.1029/2006JD007114, 2007.

Intergovernmental Panel on Climate Change (IPCC), available online at:, http://www.grida.no/publications/other/ipcc_tar/?src=/climate/ipcc_tar/, 2001.

Jacobson, M. Z.: A Physically-Based Treatment of Elemental Carbon Optics: Implications for Global Direct Forcing of Aerosols, Geophys. Res. Lett., 27(2), 217–220, 2000.

Jansen, K. L., Larson, T. V., Koenig, J. Q., Mar, T. F., Fields, C., Stewart, J., and Lippmann, M.: Associations between Health Effects and Particulate Matter and Black Carbon in Subjects with Respiratory Disease, Environ. Health Perspect., 113, 1741–1746, 2005.

Jeong, C. H., Hopke, P. K., Kim, E., and Lee, D. W.: The comparison between thermal-optical transmittance elemental carbon and Aethalometer black carbon measured at multiple monitoring sites, Atmos. Environ., 38, 5193–5204, 2004.

Jung, J. S., Lee, H., Kim, Y. J., Liu, X., Zhang, Y., Gu, J., and Fan, S.: Aerosol chemistry and the effect of aerosol water on visibility impairment and radiative forcing in Guangzhou during the 2006 Pearl River Delta campaign (PRIDE-PRD2006), J. Environ. Manage., 90, 3231–3244, 2009.

Kim, D. and Ramanathan, V.: Solar radiation budget and radiative forcing due to aerosols and clouds, J. Geophys. Res., 113, D02203, doi:10.1029/2007JD008434, 2008.

Kim, Y. J., Kim, M. J., Lee, K. H., and Park, S. S.: Investigation of carbon pollution episodes using semi-continuous instrument in Incheon, Korea, Atmos. Environ., 40, 4064–4075, 2006.

Kondo, Y., Komazaki, Y., Miyazaki, Y., Moteki, N., Takegawa, N., Kodama, D., Deguchi, S., Nogami, M., Fukuda, M., Miyakawa, T., Morino, Y., Koike, M., Sakurai, H., and Ehara, K.: Temporal variations of elemental carbon in Tokyo, J. Geophys. Res., 111, D12205, doi:10.1029/2005JD006257, 2006.

Kondo, Y., Sahu, L., Moteki, N., Khan, F., Takegawa, N., Liu, X., and Koike, M.: Consistency and traceability of black carbon measurements made by laser-induced incandescence, thermal optical transmittance, and filter-based photo-absorption technique, Aerosol Sci. Technol., in review, 2010.

Lai, S. C., Zou, S. C., Cao, J. J., Lee, S. C., and Ho, K. F.: Characterizing ionic species in PM2.5 and PM10 in four Pearl River Delta cities, South China, J. Environ. Sc., 19, 939–947, ISSN:1001-0742, CN 11-2629/X, 2007.

Latha, K. M. and Badarinath, K. V. S.: Correlation between black carbon aerosols, carbon monoxide and tropospheric ozone over a tropical urban site, Atmos. Res., 71, 265–274, 2004.

Lin, P., Hu, M., Deng, Z., Slanina, J., Han, S., Kondo, Y., Takegawa, N., Miyazaki, Y., Zhao, Y., and Sugimoto, N.: Seasonal and diurnal variations of organic carbon in PM2.5 in Beijing and the estimation of secondary organic carbon, J. Geophys. Res., 114, D00G11, doi:10.1029/2008JD010902, 2009.

Liu, X., Cheng, Y., Zhang, Y., Jung, J., Sugimoto, N., Chang, S. Y., Kim, Y. J., Fan, S., and Zeng, L.: Influences of relative humidity and particles chemical composition on aerosol scattering properties during the 2006 PRD campaign, Atmos. Environ., 42, 1525–1536, 2008.

Menon S., Hansen, J., Nazarenko, L., and Luo, Y.: Climate effects of black carbon aerosols in China and India, Science, 297, 2250–2253, doi:10.1126/science.1075159, 2002.

Miyazaki, Y., Kondo, Y., Sahu, L. K., Imaru, J., Fukushima, N, and Kano, M.: Performance of a newly designed continuous soot monitoring system (COSMOS), J. Environ. Monit., 10, 1195–1201, 2008.

Park, S. S, Kim, Y. J., and Fung, K.: PM2.5 carbon measurements in two urban areas: Seoul and Kwangju, Korea, Atmos. Environ, 36, 1287–1297, 2002

Park, S. S., Bae, M. S., Schauer, J. J., Ryu, S. S., Kim, Y. J., Cho, S. Y., and Kim, S. J.: Evaluation of the TMO and TOT methods for OC and EC measurement and their characteristics in PM2.5 at an urban site of Korea during ACE-Asia, Atmos. Environ., 39, 5101–5112, 2005.

Park, S. S., Kim, Y. J., and Kang, C. H.: Polycyclic aromatic hydrocarbons in bulk PM2.5 and size-segregated aerosol particle samples measured in an urban environment, Environ. Monit. Assess. 128, 231–240, doi:10.1007/s10661-006-9308-4, 2007.

Park, R. J., Jacob, D. J., Palmer, P. I , Clarke, A. D., Weber, R. J., Zondlo, M. A., Eisele, F. L., Bandy, A. R., Thornton, D. C., Sachse, G. W., and Bond, T. C.: Export efficiency of black carbon aerosol in continental outflow: Global implications, J. Geophys. Res., 110, D11205, doi:10.1029/2004JD005432, 2005.

Polidori, A., Turpin, B. J., Lim, H. J., Cabada, J. C., Subramanian, R., Pandis, S. N., and Robinson, A. L.: Local and Regional Secondary Organic Aerosol: Insights from a Year of Semi-Continuous Carbon Measurements at Pittsburg, Aerosol Sci. Technol., 40, 861–872, 2006.

Ramanathan, V. and Carmichael, G.: Global and regional climate changes due to black carbon, Nature Geosci., 1, 221–227, doi:10.1038/ngeo156, 2008.

Sahu, L. K., Kondo, Y., Miyazaki, Y., Kuwata, M., Koike, M., Takegawa, N., Tanimoto, H., Matsueda, H., Yoon, S. C., and Kim, Y. J.: Anthropogenic aerosols observed in Asian continental outflow at Jeju Island, Korea, in spring 2005, J. Geophys. Res., 114, D03301, doi:10.1029/2008JD010306, 2009.

Sanchez-Ccoyllo, O. R., Ynoue, R. Y., Martins, L. D., Astolfo, R., Miranda, R. M., Freitas, E. D., Borges, A. S., Fornaro, A., Freitas, H., Moreira, A., and Andrade, M. F.: Vehicular particulate matter emissions in road tunnels in Sao Paulo, Brazil, Environ. Monit. Assess., 149, 241–249, doi:10.1007/s10661-008-0198-5, 2009.

Shao, M., Tang, X., Zhang, Y., and Li, W.: City clusters in China: Air and surface water pollution, Front. Ecol. Environ., 4(7), 353–361, 2006.

Shao, M. and Zhang, Y.:Current Air quality problem and control strategies for Vehicular emissions in China, available online at: http://www.walshcarlines.com/china/china.airquality.minshao.pdf, 2001.

Streets, D. G., Bond, T. C., Carmichael, G. R., Fernandes, S. D., Fu, Q., He, D., Klimont, Z., Nelson, S. M., Tsai, N. Y., Wang, M. Q., Woo, J. H., and Yarber, K. F.: An inventory of gaseous and primary aerosol emissions in Asia in the year 2000, J. Geophys. Res., 108(D21), 8809, doi:10.1029/2002JD003093, 2003.

Suglia, S. F., Gryparis, A., Wright, R. O., Schwartz, J., and Wright, R. J.: Association of black carbon with cognition among children in a prospective birth cohort study, Am. J. Epidemiol., 167(3), 80–286, 2008.

Sugimoto, N., Nishizawa, T., Liu, X., Matsui, I., Shimizu, A., Zhang, Y., Li, R., and Liu, J.: Continuous observations of aerosol profiles with a two- wavelength Mie- cattering lidar in Guangzhou in PRD2006, J. Appl. Meteorol. Climatol., 48, 1822–1830, doi:10.1175/2009JAMC2089.1, 2009.

Takegawa, N., Kondo, Y., Koike, M., Chen, G., Machida, T., Watai, T., Blake, D. R., Streets, D. G., Woo, J. H., Carmichael, G. R., Kita, K., Miyazaki, Y., Shirai, T., Liley, J. B., and Ogawa, T.: Removal of NOx and NOy in Asian outflow plumes: Aircraft measurements over the western Pacific in January 2002, J. Geophys. Res., 109, D23S04, doi:10.1029/2004JD004866, 2004.

Takegawa, N., Miyakawa, T., Kondo, Y., Jimenez, J. L., Zhang, Q., Worsnop, D. R., and Fukuda, M.: Seasonal and diurnal variations of submicron organic aerosol in Tokyo observed using the Aerodyne aerosol mass spectrometer, J. Geophys. Res., 111, D11206, doi:10.1029/2005JD006515, 2006.

Takegawa, N., Miyakawa, T., Kuwata, M., Kondo, Y., Zhao, Y., Han, S., Kita, K., Miyazaki, Y., Deng, Z., Xiao, R., Hu, M., van Pinxteren, D., Herrmann, H., Hofzumahaus, A., Holland, F., Wahner, A., Blake, D. R., Sugimoto, N., and Zhu, T.: Variability of submicron aerosol observed at a rural site in Beijing in the summer of 2006, J. Geophys. Res., 114, D00G05, doi:10.1029/2008JD010857, 2009.

Tan, J. H., Bi, X. H., Duan, J. C., Rahn, K. A., Sheng, G. Y., and Fu, J. M.: Seasonal variation of particulate polycyclic aromatic hydrocarbons associated with PM10 in Guangzhou, China, Atmos. Res., 80, 250–262, 2006.

Turpin, B. J. and Huntzicker, J. J.: Secondary formation of organic aerosol in the Los Angeles basin: A descriptive analysis of organic and elemental carbon concentrations, Atmos. Environ., 25A, 207–215, 1991.

Turpin, B. J. and Huntzicker, J. J.: Identification of secondary organic aerosol episodes and quantitation of primary and secondary organic aerosol concentrations during SCAQS, Atmos. Environ, 29, 3527–3544, 1995.

Venkatachari, P., Zhou, L., Hopke, P. K., Schwab, J. J., Demerjian, K. L., Weimer, S., Hogrefe, Olga H., Felton, D. and Rattigan, O.: An intercomparison of measurement methods for carbonaceous aerosol in the ambient air in New York City, Aerosol Sci. Tech., 25(10), 788–795, 2006.

Westerdahl, D., Wang, X., Pan, X., and Zhang, K. M.: Characterization of on-road vehicle emission factors and microenvironmental air quality in Beijing, China, Atmos. Environ., 42, 697–705, 2009.

Xie, S, Zhang, Y., Qi, L., and Tang, X.: Spatial distribution of traffic-related pollutant concentrations in street canyons, Atmos. Environ., 37, 3213–3224, 2003.

Xiao, R., Takegawa, N., Kondo, Y., Miyazaki, Y., Miyakawa, T., Hu, M., Shao, M., Zeng, L. M., Hofzumahaus, A., Holland, F., Lu, K., Sugimoto, N, Zhao, Y., and Zhang, Y. H.: Formation of submicron sulfate and organic aerosols in the outflow from the urban region of the Pearl River Delta in China, Atmos. Environ., 43, 3754–3763, 2009.

Yang, L., Zhang, X., Gong, S., Che, H. Wang, Qu, W., and Sun, J.: Comparison of EC and BC and evaluation of dust aerosol contribution to light absorption in Xi'an, China, Environ. Monit. Assess., 120, 301–312, 2006.

Yeung, M. C., Lee, S. C., Lun, B. H., and Tanner, P. A.: Summer rain events in south-east Asia: Spatial and temporal variations, Atmos. Res., 86, 241–248, 2007.

Zhou, K., Ye, Y. H., Liu, Q., Liu, A. J., and Peng, H. L.: Evaluation of ambient air quality in Guangzhou, China, J. Environ. Sci., 19, 432–437, 2007.